Published in final edited form as:
Cell Stem Cell. 2008 February 7; 2(2): 183–189.

Transparent adult zebrafish as a tool for in vivo transplantation analysis

Richard Mark White[1,2,3], **Anna Sessa**[2], **Christopher Burke**[2], **Teresa Bowman**[2], **Jocelyn LeBlanc**[2], **Craig Ceol**[2], **Caitlin Bourque**[2], **Michael Dovey**[2,3], **Wolfram Goessling**[2,3], **Caroline Erter Burns**[4], and **Leonard I. Zon**[1,2,3]

1*Dana Farber Cancer Institute, Department of Medical Oncology, Boston, MA 02115*

2*Children's Hospital Boston, Division of Hematology/Oncology, Boston, MA 02115*

3*Harvard Medical School, Boston, MA 02115*

4*Massachusetts General Hospital, Boston, MA 02114*

Abstract

The zebrafish is a useful model for understanding normal and cancer stem cells, but analysis has been limited to embryogenesis due to the opacity of the adult fish. To address this, we have created a transparent adult zebrafish in which we transplanted either hematopoietic stem/progenitor cells or tumor cells. In a hematopoiesis radiation recovery assay, transplantation of GFP-labeled marrow cells allowed for striking *in vivo* visual assessment of engraftment from 2 hours-5 weeks post transplant. Using FACS analysis, both transparent and wild-type fish had equal engraftment, but this could only be visualized in the transparent recipient. In a tumor engraftment model, transplantation of RAS-melanoma cells allowed for visualization of tumor engraftment, proliferation and distant metastases in as little as 5 days, which is not seen in wild-type recipients until 3-4 weeks. This transparent adult zebrafish serves as the ideal combination of both sensitivity and resolution for *in vivo* stem cell analyses.

INTRODUCTION

Transplantation of hematopoietic stem cells into immunosuppressed recipients has been used over the past three decades as a treatment for diseases such as leukemia(Machida, et al, 1999). In animal models, hematopoietic stem/progenitor cell (HSPC) activity of a given population is assessed by analyzing multilineage engraftment of bone marrow or peripheral blood of recipient animals(Uchida, et al, 1994). Recently, tumor stem cells have been shown to exist for breast cancer(Al-Hajj, et al, 2003) and medulloblastoma(Singh, et al, 2004). These rare cells, which are thought to form the seed from which all other tumor cells arise, have been isolated by selecting for cells (i.e. CD133+) that can be repeatedly propagated in serial transplantation studies(Piccirillo, et al, 2006). It is evident that tumor cells undergo a homing process after transplantation(Ninomiya, et al, 2007), which is particularly dependent upon the site of transplantation. Transplantation of cancer cells, either purified or not, has long been utilized as an assay for demonstrating metastatic capacity(Gupta, et al, 2005; Yang, et al, 2004). Both HSPCs and tumor cells home to similar sites within the bone marrow vascular

Correspondence should be addressed to: Leonard I. Zon (zon@enders.tch.harvard.edu).

compartment of mice, an interaction that is critically dependent upon the SDF1-CXCR4 pathway(Sipkins, et al, 2005).

Prior work from our laboratory has demonstrated that the zebrafish is a useful model for understanding the genetics of both HSPC(Burns, et al, 2005; Traver, et al, 2004a) and tumor stem cell biology(Langenau, et al, 2007). As in murine and human systems, however, the *in vivo* spatial resolution of the adult animal is limited due to the normal opacification of skin and subdermal structures. Current *in vivo* imaging techniques, such as bioluminescence, PET, CT or MRI each have specific disadvantages in terms of resolution, sensitivity or the need for costly equipment.

Because the *in vivo* behavior of stem cell populations is considerably more complex than *in vitro* models can offer, we now describe a transparent adult zebrafish model in which the dynamics and spatial characteristics of stem cell transplantation can be fully characterized at the single cell level, in an intact *in vivo* vertebrate system that is amenable to genetic manipulation.

RESULTS

Combinatorial pigmentation mutants yield transparent adult zebrafish

The characteristic adult pigmentation pattern of the zebrafish consists of three distinct classes of pigment cells arranged in stripes (Figure 1a): black melanophores, reflective iridophores, and yellow xanthophores(Rawls, et al, 2001). The *nacre* mutant (Figure 1b) has a complete lack of melanocytes due to a mutation in the gene encoding the *mitfa* gene.(Lister, et al, 1999). The *roy orbison* (*roy*) zebrafish (Figure 1c) is a spontaneous mutant, and has a complete lack of iridophores, uniformly pigmented eyes, sparse melanocytes, and a translucency of the skin. The gene responsible for this mutant phenotype is currently unknown.

Fish that are doubly mutant for *nacre* and *roy* are shown in Figure 1d. This line, which we have named *casper* for its ghost like appearance, demonstrates a complete lack of all melanocytes and iridophores in both embryogenesis and adulthood. Most strikingly, the body of the fish is almost entirely transparent. In female adults, individual eggs are easily observable, as seen in Figure 1d. We compared the optical transparency of the *casper* line to several commonly used zebrafish pigmentation mutants, including *golden*, *albino*, *rose*, and *panther*. Organs that can be seen using standard stereomicroscopy in *casper* include the heart, aorta, intestinal tube, liver and gallbladder. Brain tissue is visible to a small extent. None of these organs are easily visible in any of the other pigment mutants studied (Supplementary Figure 1), other than the heart and intestinal tube in *rose*. Examination of the cardiac region of the *casper* mutant (Supplementary Video 1) shows that ventricular contraction can be observed, making this mutant useful for *in vivo* analysis of genetic perturbations in cardiac function. The *casper* mutant is entirely viable, with incrossed adults producing large numbers of viable offspring at expected mendelian ratios and no heterozygous phenotype.

Ocular and skin transparency is due to loss of iridophore crystals

Casper fish were sectioned and stained with hematoxylin and eosin, as well as Masson's trichrome to identify collagenous fibers. The gross morphology of the *casper* eye is normal, with maintenance of the scleral-corneal border and normal pigmented retinal epithelial cells. However, there is a complete absence of the scleral iridophore layer (Figure 2a, arrow), which is demonstrated by the loss of refractive crystalline plates(Clothier, et al, 1987) referred to as schemochromes. In wild-type animals, the pigmented retinal epithelium is normally obscured by the reflective iridophores; their absence in *roy* mutants exposes the black cells across the entire surface of the eye.

The iridophores of the skin are a dermal-hypodermal structure which are normally intimately connected to the surrounding xanthophores and lie just above the trunk skeletal muscle(Le Guellec, et al, 2004). While wild-type fish (Figure 2b, arrow) show a substantial layer of these reflective cells, the *casper* mutant has a complete absence of this layer, while the remaining skin structures are relatively intact, including epidermal scales and dermal collagen fibers as demonstrated by Masson's trichrome stain (data not shown). These data suggest that the relative transparency of the *casper* mutant is due to a combination of melanocyte loss (which normally absorbs incident light and protects subdermal structures) and iridophore loss (which normally reflect incident light away from the internal organs).

The transparent casper mutant reveals timing and homing of hematopoietic stem cells to the marrow compartment

Prior work from our laboratory has demonstrated that the transplantable hematopoietic stem/progenitor (HSPC) marrow population resides within the adult kidney, and can be isolated using flow cytometric analysis of forward and side scatter(Traver, et al, 2003). We isolated whole kidney marrow from *beta-actin:GFP* transgenic fish (which labels all cell types except red blood cells) and performed intra-cardiac (ventricular) transplantation of 100,000 whole kidney marrow cells along with 200,000 carrier red blood cells into a recipient *casper* mutant that had previously been irradiated with 25Gy. At 4 hours post transplant, a pool of blood surrounds the cardiac chambers, which likely represents extravasated blood in the pericardial sac. Within 2 weeks (Figure 3a, left), a GFP labeled population of cells is seen within the region of the zebrafish kidney as well as in the gill vasculature. By 4 weeks, a significant increase in the size and distribution of this GFP labeled population can be easily visualized, and is now largely confined to the anatomical area of the kidney of the fish (Figure 3b, right). For comparison, a wild-type fish transplanted in an identical manner is shown, demonstrating that essentially no GFP can normally be seen in an opaque adult. These data suggest that the transparent *casper* mutant allows for ready visualization of hematopoietic progenitor engraftment after a sublethal dose of 25Gy, consistent with short-term hematopoietic engraftment.

The kidneys were dissected from the 4 week post transplant fish (both *casper* and wild-type) and analyzed for their forward/side scatter profile as well as GFP. Although no GFP can be visualized with a fluorescent stereoscope in the wild-type, a normal distribution of hematopoietic cells is seen at 4 weeks post transplant, and many of these cells are GFP positive (Figure 3b, top). Based on the scatter profile, multilineage engraftment has occurred, which indicates that the engrafted cells represent a primitive hematopoietic population. The kidney from the *casper* mutant shows a similar reconstitution of hematopoietic lineages which are also GFP positive, to the same degree (Figure 3b, bottom). These data demonstrate that the anatomic localization of GFP positive cells in the *casper* mutant is indeed indicative of marrow reconstitution.

Recipient fish at 4 weeks post transplant were fixed and processed for H&E and anti-GFP IHC. Kidney sections shows large numbers of hematopoietic cells (H)surrounding the tubules (T) and glomeruli (G) of the kidney (Figure 3c, left), consistent with previous observations(Traver, et al, 2004b). All of the hematopoietic cells are strongly GFP-positive by IHC (Figure 3c, right - brown staining), whereas none of the kidney tubule cells stain for GFP. This confirms the proper homing of the GFP-labeled marrow cells back to the kidney marrow of the recipient *casper* fish.

Because one of the major advantages of an optically clear adult animal is the ability to achieve single-cell resolution in a live animal, we next used confocal microscopy on adult zebrafish that had been transplanted with beta-actin GFP HSPCs 4 weeks earlier. Imaging of a transplanted wild-type recipient yielded no discernable GFP signal due to the opacity of the

normal skin. In contrast, the *casper* mutant allowed for identification of cells both singly and in clusters (Figure 3d) at a resolution of approximately 5 um. The maximal depth of field achieved with a Zeiss confocal microscope was 88um from the surface of the skin.

To ensure that the *casper* mutant will be generally applicable to stem cell biologists, we measured survival after HSPC transplant in wild-type and *casper* recipients. As shown in Figure 3e, although both groups show an initial procedural mortality, there is no significant difference in survival between the groups, indicating that *casper* will function similarly to wild-type animals in transplant studies.

The casper mutant allows for rapid identification of transplanted tumor cells

We next assessed whether the transparent *casper* zebrafish could be used to analyze *in vivo* tumor engraftment and migration after transplantation. Stable transgenic zebrafish carrying either the mutated human B-raf or N-ras-GFP fusion oncogene under the control of the melanocyte specific *mitf* promoter were crossed to $p53^{-/-}$ fish. These fish reliably develop highly aggressive melanoma in 4-12 months. A tumor from an adult fish was disaggregated into a single cell suspension and 200,000 cells were transplanted either into the ventral peritoneum (IP) or via intra-ventricular (IC) injection into an irradiated *casper* recipient. Within 5 days post IP transplantation of the NRAS-GFP melanoma (Figure 4a, top), a large mass of deeply pigmented tumor cells could be visualized within the peritoneum. In addition, a small number of cells have localized to the dorsal epidermal scales (Figure 4a, top, circled). The pattern of engraftment at 5 days in the intra-cardiac recipients of NRAS-GFP cells (Figure 4a, bottom) largely reflects local deposition of tumor cells along the transplantation tract, although some cells can be seen migrating dorsally. The inset of Figure 4a (bottom) demonstrates that the tumor cells (taken at 10 days post transplant) continue to be strongly GFP positive and indicates that they could be localized even in the absence of black pigmentation. In Figure 4b, a large mass is seen 14 days after IP transplantation of 200,000 BRAF;p53 melanoma. Mediolateral and ventral views of this tumor allow for 3-dimensional calculation of tumor volume (in this case $1496mm^3$). The ability to calculate 3-D tumor volume and whole body distribution of tumor cells provides an important quantitative analysis of engraftment after small numbers of tumor cells, and offers the potential for monitoring *in vivo* effects of therapeutically useful molecules.

We repeatedly imaged a single recipient fish over a period of 4 weeks using standard stereomicroscopy in order to quantify tumor growth over time. As shown in Figure 4c, this individual fish is fully viable over this period of time, and the tumor volume can be assessed at each time point without sacrificing the animal. Because non-melanized, but fluorescently labeled tumor cells can be visualized in the same manner, this tumor transplant model should be amenable to virtually any transplantable tumor.

Finally, to explore the utility of *casper* as a tool in understanding metastatic progression, we examined each fish that had been transplanted with BRAF;p53 melanoma cells for evidence of tumor dissemination. Between 5 and 28 days post transplant, 9/24 (37.5%) of all transplant recipients had evidence of distant metastasis, with the peak of initial dissemination occurring between 5 and 10 days. In Figure 4d, two representative fish are shown, with the initial site of implantation demonstrated by the arrow. In the left-hand figure, very widespread dissemination is seen throughout the animal, both as single cells as well as in clusters of cells. In the right-hand figure, a small cluster of individual cells (see inset) have disseminated far away from the implantation site and have become embedded in the dorsal skin. At least one of these cells has the stellate appearance of a migratory melanoma cell. Because there are no pigmented cells between the primary mass and this single dorsal cell, this supports the concept that these cells represent dissemination from the primary transplant. In a similarly transplanted wild-type fish, no visible tumors are seen until 2-3 weeks post transplant, and metastatic cells are not

detectable. Although the mechanism of such early and widespread dissemination is unclear at this point, it may represent the accumulation of complex genetic changes in the BRAF;p53 donor cells, since the donor tumors had been present for well over a month. In the future, we plan on studying the factors that determine the capacity for transplanted cells to undergo early dissemination, as well as the mechanism of the "switch" between disseminated micrometastatic disease and bulk macrometastases.

DISCUSSION

The casper mutant as a model for *in vivo* imaging of stem cell and tumor biology

The data presented here demonstrate that the optical properties of the *casper* fish offers a unique combination of high resolution (~5um),sensitivity and amenability to deep tissue imaging with commonly available laboratory equipment. Although similar to the "see through" medaka strain(Wakamatsu, et al, 2001), the zebrafish has become a more commonly utilized tool for studying stem cell and tumor biology, and should be broadly applicable to stem cell researchers. One limitation of this line is that it requires that both mutations (*nacre* and *roy*) be present in the homozygous state, which will require at least 2 breeding cycles to take advantage of currently available transgenic lines. In addition, because the mutation in *roy* is currently unknown (but under active investigation), it is possible that this gene defect may affect some unknown aspects of tumor or stem cell biology, although it clearly does not affect survival. Identification of the *roy* defect will help clarify this point. Finally, imaging of very deep tissues may require multi-photon microscopy, which is currently experimental in the zebrafish system.

Comparison of the transparent zebrafish to currently available *in vivo* imaging techniques

In vivo imaging is a critical counterpart to studying molecular processes in cell culture systems (Koo, et al, 2006). The goal of all imaging techniques is to combine resolution (i.e. single or subcellular) with sensitivity (whole-animal or organ) to gain a comprehensive understanding of processes that have unique *in vivo* behavior, such as tumor metastasis and stem cell homing. Current *in vivo* imaging of small animals consists of several techniques, summarized in Supplementary Table 1, that are often used in complement.

Bioluminescence has been utilized to detect engraftment and hematopoietic reconstitution after transplantation of luciferase-positive HSC populations(Welsh, et al, 2005;Cao, et al, 2006). Although bioluminescence had high sensitivity in this study, it had limited spatial resolution (on the order of 1-10mm), required several minutes of imaging per animal, detection of light from deep tissues is limited, and requires intravenous administration of substrate. Whole animal imaging using bioluminescent marking of transplanted tumor cells has the capacity to give broad pictures of tumor metastasis using cells such as uveal melanoma(Notting, et al, 2005) or lung cancers(Zacharakis, et al, 2005) but the sensitivity of this technique is somewhat limited in metastasis, since bioluminescent evidence of metastatic spread can take 4 weeks or more to detect. Our ability to detect clearly evident metastases in as few as 3-5 days is unique amongst vertebrate models, and the resolution is such that single metastatic cells can be easily visualized using standard stereomicroscopes. In addition, bioluminescence has met with only limited success in the zebrafish system(Creton, et al, 1997; Kaneko, et al, 2005).

Fluorescent imaging is widely available and is a standard method of analysis of gene function in zebrafish embryos; image acquisition is rapid, but is of limited use in adult wild-type zebrafish. Our data indicate that the useful range of the stereomicroscope can be considerably extended to the adult fish, in both the visible and fluorescent ranges, due to the optical clarity of our model. When combined with confocal microscopy, single cell resolution is easily achievable, and the use of dual-photon confocal microscopy is likely to yield much greater depth of image resolution in the *casper* line. Crossing the *casper* line to the numerous transgenic

lines that label vasculature (i.e. fli-GFP, shown in Supplementary Figure 2) or internal organs with fluorescent tags (i.e. pdx-GFP for pancreas, LFABP-GFP for liver) may be of considerable use to those interested in *in vivo* analysis of angiogenesis, organ homeostasis and regeneration after injury. However, direct injection of transgenic constructs in the *casper* background may be advantageous since it eliminates the need for complex breeding strategies to maintain double homozygosity of *roy* and *nacre*.

Although microCT, MRI and PET scans each have considerable advantages in terms of whole-body imaging, they all require highly specialized equipment, significant optimization, and intravenous contrast agents. MRI is a useful technique for visualizing transplanted cells *in vivo*, and has a spatial resolution of 25-50um, but requires a significant amount of magnetic dye treatment of transplanted cells, has limited sensitivity, and requires considerably complex and expensive equipment(Lee, et al, 2007; Lyons, 2005). PET imaging, which can detect relatively small numbers of tumor cells, requires radioactive labeling of cell populations, is only moderately sensitive and necessitates small animal PET scanners, which are not broadly available(Beckmann, et al, 2007; Tai, et al, 2005). Another concern is the dose of radiation in both CT and PET that would need to be delivered to the fish to achieve adequate resolution, which may have independent biological effects(Paulus, et al, 2000; Pickhardt, et al, 2005). Although each of these techniques will likely have a future role in zebrafish imaging, none currently offers the rapidity, cellular resolution and sensitivity that fluorescent microscopy that is achievable in the *casper* zebrafish.

Future applications

The development of a robust, fertile and easily maintained transparent adult zebrafish provides an important adult complement to the studies that are achievable in the transparent zebrafish embryo. Our data suggests that the *casper* fish will serve as a useful platform for researchers interested in processes such as stem cell engraftment and homing. For cancer biologists, it opens a window onto longitudinal analysis of tumor growth, invasion, metastases and angiogenesis, at an anatomic resolution not readily achievable in murine or other systems. When combined with transgenic lines that label structures such as the vasculature (i.e. *fli*-GFP) or epithelium (i.e. *keratin*-GFP), a detailed understanding of the manner in which individual stem cells interact with their endogenous niche can be analyzed. Because the adult zebrafish is well suited to genetic and small molecule based screens, the *casper* fish will allow for detailed *in vivo* study of stem and cancer biology in a vertebrate organism with great relevance to human biology.

MATERIALS AND METHODS

Zebrafish husbandry

Zebrafish were bred and maintained in the Karp fish facility, in temperature (28C), pH (7.4) and salinity controlled conditions. All fish were maintained in a 14h on/10h off light cycle.

Generation of compound mutant lines

Lines used in these studies included wild-type (AB), tg(beta-actin:GFP) kindly provided by Ken Poss, roy orbison (provided by the Dowling lab at Harvard), panther/rose (provided by the Parichy lab at university of Washington), nacre (provider by the Lister lab at Virginia Commonwealth University). The p53, golden and albino lines are maintained in our laboratory, as previously described. The tg(*mitf:NRAS-GFP*) line was developed by Michael Dovey in the Zon laboratory (manuscript in preparation). The tg(mitf:BRAF) line was described previously.

In vivo microscopy

Adult animals were anesthetized with 0.2% Tricaine in E3 fish water. After mounting on a fixed plastic or agarose plate, whole animal images were taken with a Nikon D200 digital camera using an adjustable flash system. For fluorescent and magnification views, a Zeiss Discovery V8 stereomicroscope with a 1.2X PlanApo lens and GFP/RFP filters was used. Images were captured using Zeiss proprietary software and analyzed using ImageJ.

Confocal microscopy

Transplant recipient zebrafish were embedded in 1% low-melting point agarose containing 0.04 mg/ml Tricaine-S in glass-bottom culture dishes. Confocal microscopy was performed for GFP positive cells using a Zeiss LSM Meta confocal microscope.

Histological analysis

Adult fish were fixed in 4% paraformaldehyde overnight. After processing and paraffin embedding, 5um sections were cut in either longitudinal or transverse sections. Staining was done with either hematoxylin and eosin or Masson's trichrome for collagen analysis. For immunohistochemistry, sections were counterstained with eosin and stained using an anti-GFP antibody (Upstate, catalog #06-896)

Zebrafish whole kidney marrow transplantation

Hematopoietic transplantation was done as previously described, with the following modifications. Whole kidneys from beta actin:GFP donor fish were dissected using forceps and placed in 0.9X PBS/5% FCS. Manual disaggregation using a P1000 pipette resulted in single cell suspensions. Cells were filtered over a 40um nylon mesh filter, and resuspended in PBS/FCS to give a final concentration of 100,000 cells/ul.

Recipient fish were irradiated with 25Gy of gamma irradiation 2 days prior to transplantation, and allowed to recover in standard fish water. On the day of transplant, recipients were anesthetized in 0.2% Tricaine. Using a Hamilton syringe, 5ul of cell suspension was transplanted into the cardiac chamber and the fish immediately returned to fresh fish water. Recipients were kept off of system water (to minimize infectious risk) for 1 week and fed standard flake/brine shrimp meals.

FACS analysis of recipient kidney marrow

At 4 weeks post transplant, recipient fish were sacrificed with an overdose of tricaine and kidney marrow cells isolated as above. FACS sorting of single cells were analyzed for forward/side scatter profiles as well as GFP fluorescence. FACS data was analyzed using FloJo software.

Zebrafish melanoma transplantation

A single melanoma from a stable tg(mitf:NRAS-GFP);$p53^{-/-}$ or tg(mitf:BRAF);$p53^{-/-}$ adult was dissected from from skin and underlying connective tissue, and placed in a dish with 100ul of 0.9XPBS/0.1mg/ml Liberase). The tumor was minced and manually disaggregated with razor blades, with additional Liberase solution applied as need to maintain hydration. After 1hr of digestion, the reaction was stopped by the addition of 5%FCS. The cell suspension was filtered as above and resuspended to a final concentration of 50,000 cells/ul. Cells were transplanted into previously irradiated recipients, as above, using 5ul into either the peritoneal cavity of via intracardiac injection.

Supplementary Material

Refer to Web version on PubMed Central for supplementary material.

Acknowledgements

The authors wish to thank Sara Henry, who provided initial inspiration towards the creation of a transparent zebrafish. Dr. Lois Smith of the Department of Ophthalmology at Children's Hospital Boston offered expert advice on the analysis of the *roy* eye defect. Alan Flint assisted with flow analysis of zebrafish kidney marrow. R.M.W. was supported by an ASCO YIA Grant and the Aid for Cancer Research. L.I.Z. was supported by the Howard Hughes Medical Institution and National Institutes for Health.

Reference List

Al-Hajj M, Wicha MS, Benito-Hernandez A, Morrison SJ, Clarke MF. Prospective identification of tumorigenic breast cancer cells. Proceedings of the National Academy of Sciences of the United States of America 2003;100:3983–8. [PubMed: 12629218]

Beckmann N, Kneuer R, Gremlich HU, Karmouty-Quintana H, Ble FX, Muller M. In vivo mouse imaging and spectroscopy in drug discovery. NMR Biomed 2007;20:154–185. [PubMed: 17451175]

Burns CE, Traver D, Mayhall E, Shepard JL, Zon LI. Hematopoietic stem cell fate is established by the Notch-Runx pathway. Genes & Development 2005;19:2331–42. [PubMed: 16166372]

Cao F, Lin S, Xie X, Ray P, Patel M, Zhang X, Drukker M, Dylla SJ, Connolly AJ, Chen X, et al. In vivo visualization of embryonic stem cell survival, proliferation, and migration after cardiac delivery. Circulation 2006;113:1005–1014. [PubMed: 16476845]

Clothier J, Lythgoe JN. Light-induced colour changes by the iridophores of the Neon tetra, Paracheirodon innesi. J. Cell. Sci 1987;88(Pt 5):663–668. [PubMed: 3503061]

Creton R, Steele ME, Jaffe LF. Expression of apo-aequorin during embryonic development; how much is needed for calcium imaging? Cell Calcium 1997;22:439–446. [PubMed: 9502193]

Dickson PV, Hamner B, Ng CY, Hall MM, Zhou J, Hargrove PW, McCarville MB, Davidoff AM. In vivo bioluminescence imaging for early detection and monitoring of disease progression in a murine model of neuroblastoma. J. Pediatr. Surg 2007;42:1172–1179. [PubMed: 17618876]

Goessling W, North TE, Zon LI. Ultrasound biomicroscopy permits in vivo characterization of zebrafish liver tumors. Nat. Methods 2007;4:551–553. [PubMed: 17572681]

Gupta PB, Kuperwasser C, Brunet JP, Ramaswamy S, Kuo WL, Gray JW, Naber SP, Weinberg RA. The melanocyte differentiation program predisposes to metastasis after neoplastic transformation. Nature Genetics 2005;37:1047–54. [PubMed: 16142232]

Kaneko M, Cahill GM. Light-dependent development of circadian gene expression in transgenic zebrafish. PLoS Biol 2005;3:e34. [PubMed: 15685291]

Koo V, Hamilton PW, Williamson K. Non-invasive in vivo imaging in small animal research. Cell. Oncol 2006;28:127–139. [PubMed: 16988468]

Le Guellec D, Morvan-Dubois G, Sire JY. Skin development in bony fish with particular emphasis on collagen deposition in the dermis of the zebrafish (Danio rerio). Int. J. Dev. Biol 2004;48:217–231. [PubMed: 15272388]

Lee JH, Huh YM, Jun YW, Seo JW, Jang JT, Song HT, Kim S, Cho EJ, Yoon HG, Suh JS, Cheon J. Artificially engineered magnetic nanoparticles for ultra-sensitive molecular imaging. Nat. Med 2007;13:95–99. [PubMed: 17187073]

Lister JA, Robertson CP, Lepage T, Johnson SL, Raible DW. Nacre Encodes a Zebrafish Microphthalmia-Related Protein that Regulates Neural-Crest-Derived Pigment Cell Fate. Development 1999;126:3757–3767. [PubMed: 10433906]

Lyons SK. Advances in imaging mouse tumour models in vivo. J. Pathol 2005;205:194–205. [PubMed: 15641018]

Machida U, Kami M, Hirai H. Hematopoietic stem-cell transplantation for acute leukemia. The New England Journal of Medicine 1999;340:810. [PubMed: 10075530]author reply 811-2

Ninomiya M, Abe A, Katsumi A, Xu J, Ito M, Arai F, Suda T, Ito M, Kiyoi H, Kinoshita T, Naoe T. Homing, proliferation and survival sites of human leukemia cells in vivo in immunodeficient mice. Leukemia 2007;21:136–142. [PubMed: 17039228]

Notting IC, Buijs JT, Que I, Mintardjo RE, van der Horst G, Karperien M, Missotten GS, Jager MJ, Schalij-Delfos NE, Keunen JE, van der Pluijm G. Whole-body bioluminescent imaging of human uveal melanoma in a new mouse model of local tumor growth and metastasis. Investigative Ophthalmology & Visual Science 2005;46:1581–7. [PubMed: 15851554]

Paulus MJ, Gleason SS, Kennel SJ, Hunsicker PR, Johnson DK. High resolution X-ray computed tomography: an emerging tool for small animal cancer research. Neoplasia 2000;2:62–70. [PubMed: 10933069]

Piccirillo SG, Reynolds BA, Zanetti N, Lamorte G, Binda E, Broggi G, Brem H, Olivi A, Dimeco F, Vescovi AL. Bone morphogenetic proteins inhibit the tumorigenic potential of human brain tumour-initiating cells. Nature 2006;444:761–5. [PubMed: 17151667]

Pickhardt PJ, Halberg RB, Taylor AJ, Durkee BY, Fine J, Lee FT Jr, Weichert JP. Microcomputed tomography colonography for polyp detection in an in vivo mouse tumor model. Proc. Natl. Acad. Sci. U. S. A 2005;102:3419–3422. [PubMed: 15728368]

Rawls JF, Mellgren EM, Johnson SL. How the zebrafish gets its stripes. Dev. Biol 2001;240:301–314. [PubMed: 11784065]

Singh SK, Hawkins C, Clarke ID, Squire JA, Bayani J, Hide T, Henkelman RM, Cusimano MD, Dirks PB. Identification of human brain tumour initiating cells. Nature 2004;432:396–401. [PubMed: 15549107]

Sipkins DA, Wei X, Wu JW, Runnels JM, Cote D, Means TK, Luster AD, Scadden DT, Lin CP. In vivo imaging of specialized bone marrow endothelial microdomains for tumour engraftment. Nature 2005;435:969–73. [PubMed: 15959517]

Tai YC, Ruangma A, Rowland D, Siegel S, Newport DF, Chow PL, Laforest R. Performance evaluation of the microPET focus: a third-generation microPET scanner dedicated to animal imaging. J. Nucl. Med 2005;46:455–463. [PubMed: 15750159]

Traver D, Paw BH, Poss KD, Penberthy WT, Lin S, Zon LI. Transplantation and in vivo imaging of multilineage engraftment in zebrafish bloodless mutants. Nature Immunology 2003;4:1238–46. [PubMed: 14608381]

Traver D, Winzeler A, Stern HM, Mayhall EA, Langenau DM, Kutok JL, Look AT, Zon LI. Effects of lethal irradiation in zebrafish and rescue by hematopoietic cell transplantation. Blood 2004a; 104:1298–305. [PubMed: 15142873]

Traver D, Winzeler A, Stern HM, Mayhall EA, Langenau DM, Kutok JL, Look AT, Zon LI. Effects of lethal irradiation in zebrafish and rescue by hematopoietic cell transplantation. Blood 2004b; 104:1298–305. [PubMed: 15142873]

Uchida N, Aguila HL, Fleming WH, Jerabek L, Weissman IL. Rapid and sustained hematopoietic recovery in lethally irradiated mice transplanted with purified Thy-1.1lo Lin-Sca-1+ hematopoietic stem cells. Blood 1994;83:3758–79. [PubMed: 7911343]

Wakamatsu Y, Pristyazhnyuk S, Kinoshita M, Tanaka M, Ozato K. The see-through medaka: a fish model that is transparent throughout life. Proc. Natl. Acad. Sci. U. S. A 2001;98:10046–10050. [PubMed: 11526229]

Welsh DK, Kay SA. Bioluminescence imaging in living organisms. Curr. Opin. Biotechnol 2005;16:73–78. [PubMed: 15722018]

Yang J, Mani SA, Donaher JL, Ramaswamy S, Itzykson RA, Come C, Savagner P, Gitelman I, Richardson A, Weinberg RA. Twist, a master regulator of morphogenesis, plays an essential role in tumor metastasis. Cell 2004;117:927–39. [PubMed: 15210113]

Zacharakis G, Kambara H, Shih H, Ripoll J, Grimm J, Saeki Y, Weissleder R, Ntziachristos V. Volumetric tomography of fluorescent proteins through small animals in vivo. Proceedings of the National Academy of Sciences of the United States of America 2005;102:18252–7. [PubMed: 16344470]

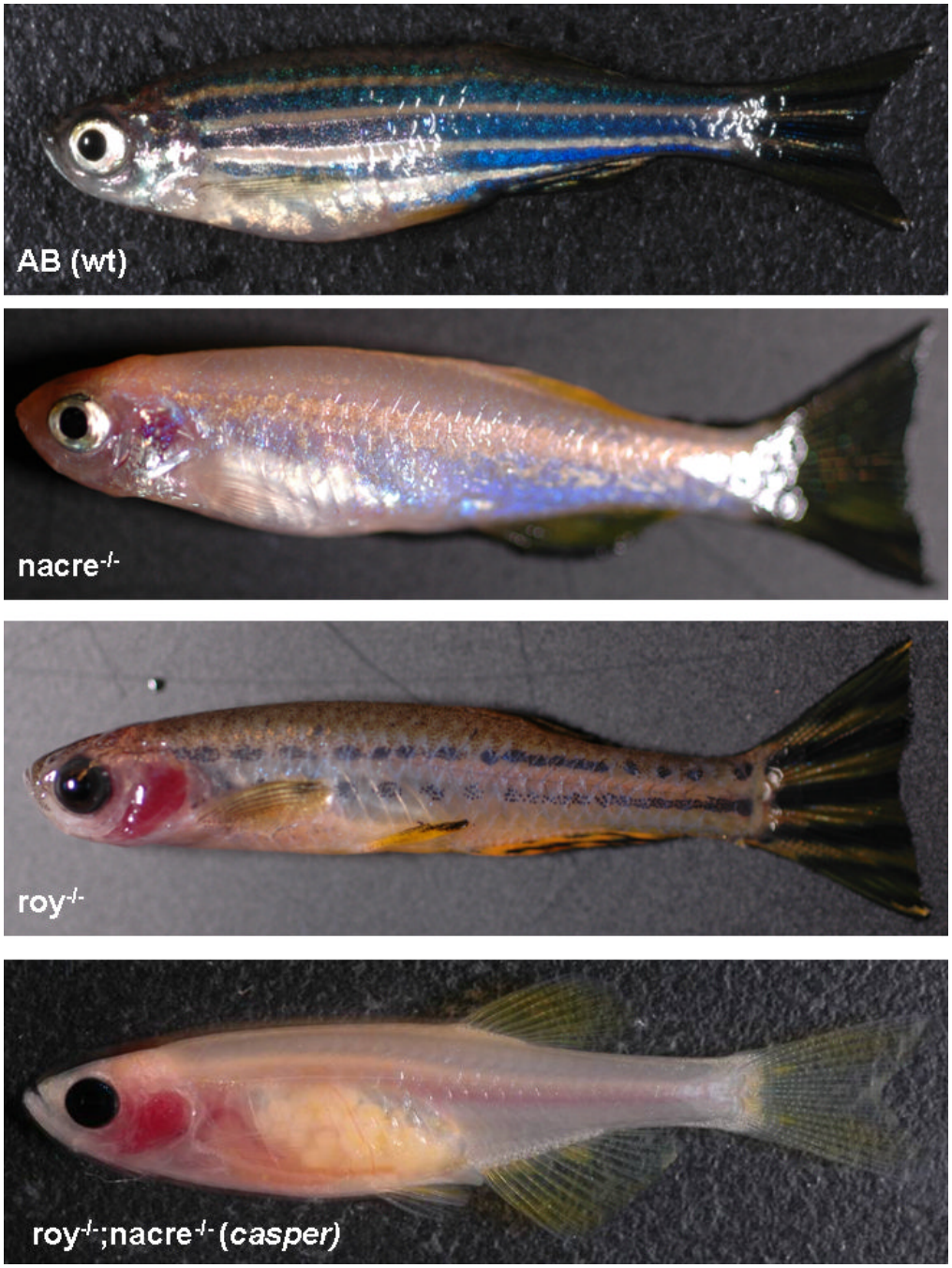

Figure 1.

Zebrafish pigmentation mutants exhibit defects in specific neural crest derived populations. A wild-type zebrafish (1A) demonstrates alternating patterns of deeply pigmented stripes comprised largely of melanocytes. The interstripe regions, devoid of melanocytes, contain primarily reflective iridophores and yellowish xanthophores. The *nacre* mutant (1B), due to loss of *mitf*, shows a loss of embryonic and adult melanocytes, with a compensatory increase in iridophore numbers. The *roy orbison* mutant (1C), whose genetic defect is currently undefined, shows a striking abnormality of eye pigmentation, a severe disruption of melanocyte numbers/patterning, and a complete loss of the iridophore layer. The compound *roy;nacre* double homozygous mutant (1D), which we have named *casper*, shows the effect of combined

melanocyte and iridophore loss, in which the body of the adult fish is largely transparent due to loss of light absorption and reflection.

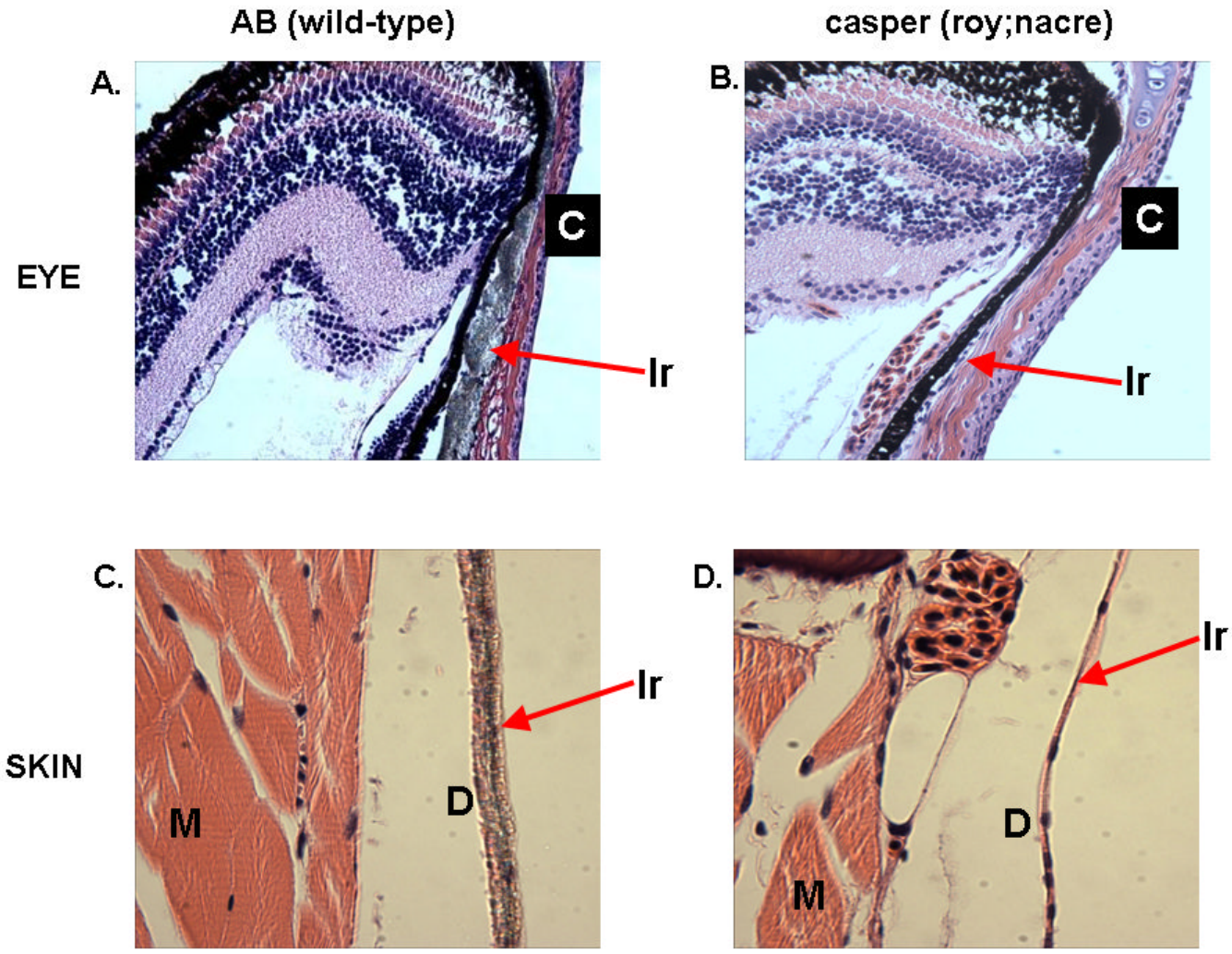

Figure 2.

Transverse section of wild-type (2A) and casper *(roy;nacre)* eyes (2B) demonstrates that the uniformly pigmented eye in the mutant line is primarily due to a loss of reflective iridophores in the sclera (arrow shows iridophores in wild-type fish), which then exposes the black underlying pigmented retinal epithelium. The remaining eye structures appear intact. Transverse sectioning of the adult skin from wild-type (2C) and *casper* (2D) shows a thick layer of iridophore crystals in the hypodermis of the wild-type adult (arrow) but a complete loss of this cell layer in the *casper* skin. Light that would normally be intercepted by epidermal/dermal melanocytes can penetrate deeply into the hypodermis of the mutant, and is not reflected away due to the lack of iridophore crystals. This allows for deep tissue penetration of normal wavelength length. M=muscle layer; D=dermis; Ir=iridophores, C=corneal surface.

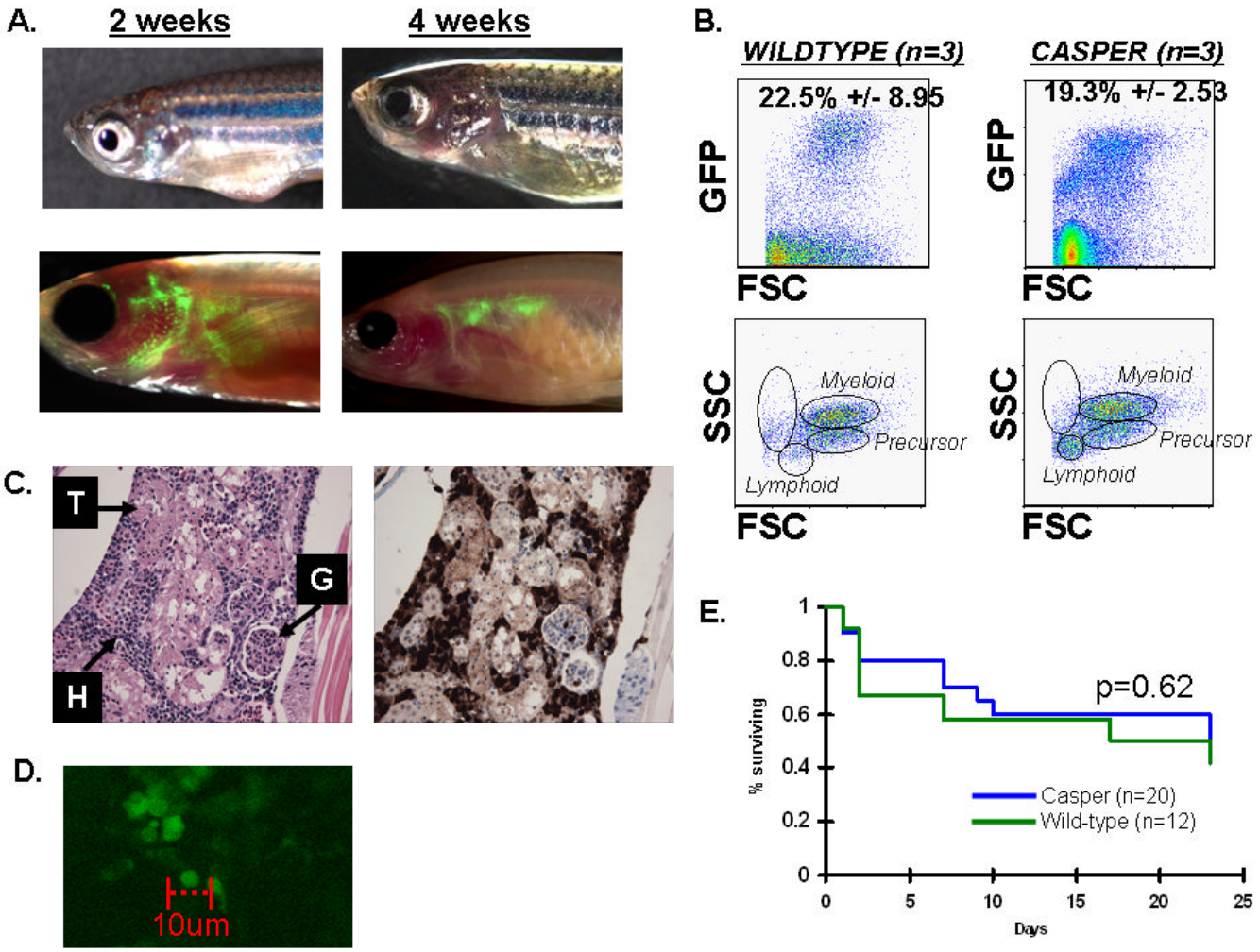

Figure 3.

Whole kidney marrow from beta actin:GFP labeled donors was transplanted into either wild-type (n=6) or *casper* (n=6) irradiated recipients via intra-cardiac (IC) injection of 100,000 cells. Fish were imaged from 4 hours until 5 weeks post transplant at once weekly intervals. At 2 weeks (3A, left), GFP positive cells can be seen to circulate and home to the region near the gills and head kidney of the recipient only in the *casper* line. By 4 weeks (3A, right), a population of GFP positive cells is tightly localized to the zebrafish kidney, where most adult hematopoietic tissue is known to reside. The GFP positive cells can only been seen in the transparent *casper* recipient. To confirm that the GFP labeled cells represented true hematopoietic cells, whole kidney was isolated from wild-type and *casper* recipients at 4 weeks, and subject to FACS analysis (3B). Both the wild-type (3B, left) and transparent mutant (3B, right) repopulated their kidney marrow with a full repertoire of hematopoietic lineages. In both types of recipients, a subset of the sorted cells were GFP positive (19-22%), as is expected in a mosaic transplantation assay. In (3C), histological analysis of the *casper* transplant recipient is shown at 4 weeks post transplant. H&E staining (3C, left) shows a robust population of hematopoietic cells (labeled “H”) intertwined with normal kidney glomeruli (labeled “G”) and tubules (labeled “T”). Immunohistochemistry using an anti-GFP antibody (3C, right) demonstrates that only the hematopoietic cells are strongly GFP positive (brown staining) whereas the kidney tubules and glomeruli are negative. Confocal laser scanning was used to examine a transplant recipient at 4 weeks post transplant (4D), and demonstrates easily

discernible single GFP positive cells in the kidney marrow space. Survival after transplantation was identical in wild-type versus *casper* mutants (4E).

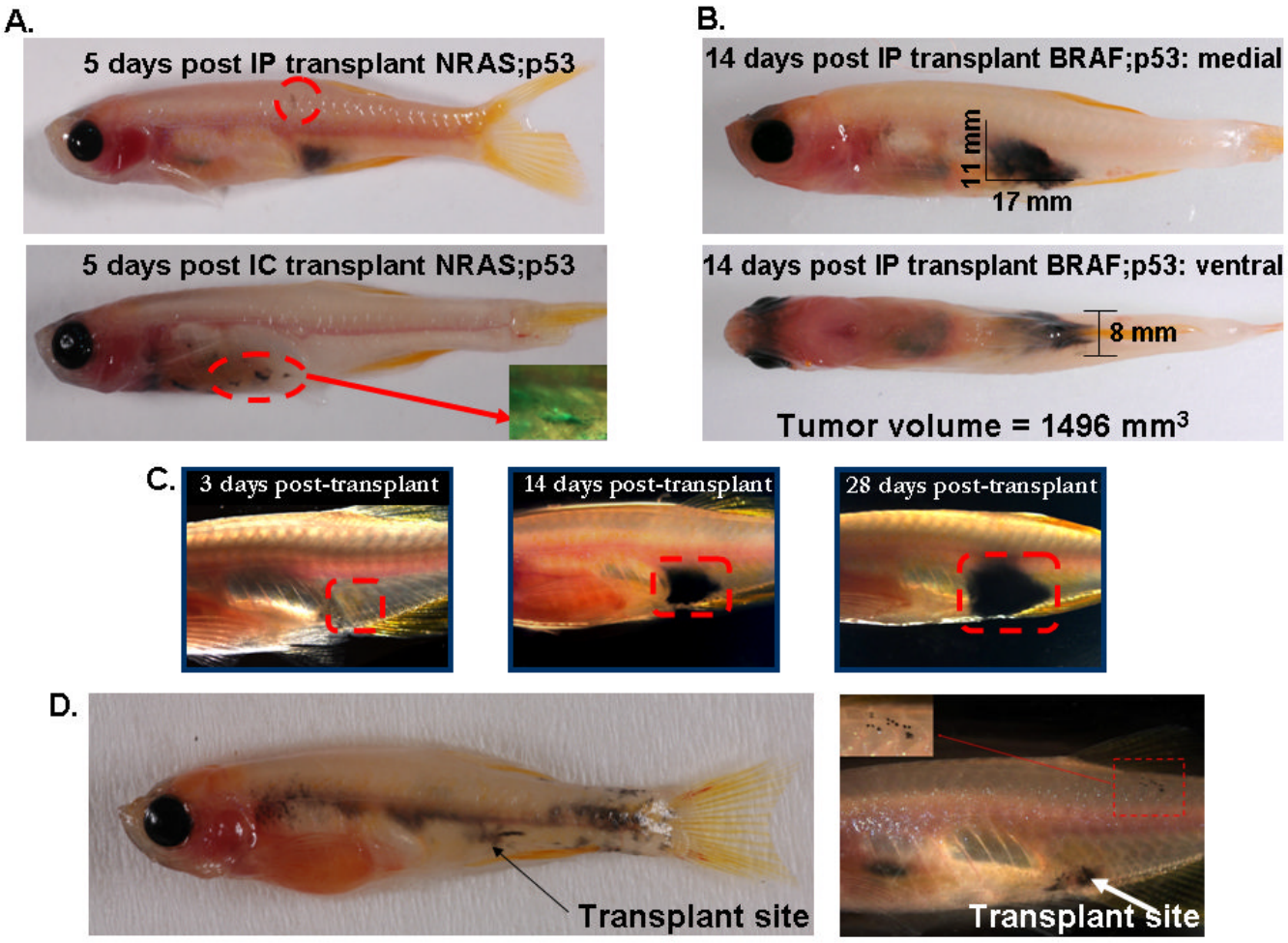

Figure 4.

mitf-NRAS-GFP;p53$^{-/-}$(4A) driven melanoma cells were transplanted into *casper* adults into either the peritoneum (IP, n=6) or via intracardiac injection (IC, n=5) at a dose of 200,000 cells. By 5 days post IP transplant of NRAS-GFP cells (4A, top), a large deeply pigmented intra-abdominal mass could be seen (n=3/6 fish) as well as spread to the dorsal epidermal scales (circled area). After IC injection of NRAS-GFP cells (4A, bottom), the cells proliferated and enlarged along the needle tract but did not appear to spread to distant sites. The inset, taken at 10 days post-transplant, shows that the cells continue to be strongly GFP positive. In Figure 4B, IP transplantation of *mitf*-BRAF;p53$^{-/-}$ melanoma cells demonstrates 14 day engraftment within the peritoneal cavity. Mediolateral and ventral views allow for calculation of 3-dimensional tumor volume. In 4C, repeated imaging of the same fish over a 1 month period demonstrates gradual increase in tumor volume without the need for sacrifice of the recipient. In a study of 24 transplant recipient fish, 37.5% were found to develop distant metastasis, examples of which are shown in 4D. Single migratory (stellate appearing) melanoma cells (4D, right, inset box) have migrated far from the transplantation site and embedded in the dorsal skin.